Ion-size dependences of the salting-out effect: Reversed order of sodium and lithium ions

Hiroyuki Katsuto,[†,‡] Ryuichi Okamoto,[†,‡] Tomonari Sumi,[†,‡] and Kenichiro Koga[*,†,‡]

†*Research Institute for Interdisciplinary Science, Okayama University, Okayama 700-8530, Japan*

‡*Department of Chemistry, Faculty of Science, Okayama University, Okayama 700-8530, Japan*

E-mail: koga@okayama-u.ac.jp

May 24, 2021

Abstract

A general trend of the salting-out effect on hydrophobic solutes in aqueous solution is that the smaller the size of a dissolved ion the larger the effect of reducing the solubility of a hydrophobe. An exception is that Li^+, the smallest in alkali metal ions, has a notably weaker effect than Na^+. To understand the reverse order in the cation series, we performed molecular dynamics simulations of aqueous solutions of salt ions and calculated the Setschenow coefficient of methane with the ionic radius of either a cation or an anion varied in a wide range. It is confirmed that the Setschenow coefficient is correlated with the packing fraction of salt solution, as observed in earlier studies, and also correlated with the partial molar volume of an ion. Analyses of correlation-function integrals, packing fractions of solvation spheres, and orientations of water molecules surrounding an ion reveal the key differences in microscopic properties between the cation and anion series which give rise to the reverse order in the cation series of the partial molar volumes of ions and ultimately that of the Setschenow coefficients.

Introduction

Adding salt to water often enhances the hydrophobic effect, thereby further decreasing the solubilities of gases and hydrocarbons in water or making otherwise perfectly miscible components partially miscible (the salting out); some ionic species may induce the opposite effect (the salting in). Whether the salting-out or salting-in effect manifests itself, and how strong it is, depends on both ionic and solute species: experimental data are available for combinations of common ions and relatively simple solute species.[1–4] Molecular theory has yet to be developed in order to understand the law of the salting-out effect.[5] Salt effects on the solubility of biological molecules such as peptides and proteins, and the effects on effective interactions between those molecules, are one of the challenging subjects in physical chemistry: Recent experimental and computer simulation studies provided detailed pictures of

specific interactions of ions with proteins, thereby promoting a molecular level understanding of the Hofmeister series.[6–10] Hydrophobic and hydrophilic moieties in biological molecules are the two key factors determining their solubility, and therefore clarifying independently ion specific effects on each group should also form a basis necessary to fully understand the Hofmeister ordering. Here we focus the ion size effect on the solubility of small, nonpolar molecules in aqueous solution, which has been a subject of earlier theoretical studies[11–18] but has not yet fully understood. It is well known that the salting-out ability becomes weaker as either the cation or anion size increases while the opposite species is fixed; a notable exception is found in a series of alkali metal ions where the salting-out effect peaks at Na^+ and the effect of Li^+ is as weak as that of Cs^+.

In his pioneering work, J. Setschenow proposed and verified that the solubility of a gas in aqueous electrolyte solution varies exponentially with the salt concentration.[19] That is, in the present notation,

$$\frac{\lambda}{\lambda_0} = \mathrm{e}^{-K_s \rho}, \tag{1}$$

where λ and λ_0 are the Ostwald absorption coefficients of the gas in aqueous solution and in pure water, respectively, and ρ is the number density of the electrolyte; K_s is called the Setschenow (Sechenov) coefficient, a measure of the salting-out effect which is specific to both ionic and solute species. Commonly used today is $k_{\mathrm{scc}} = -(1/c_s)\log_{10}[\lambda/\lambda_0]$ with c_s the molar concentration of salt.[2] In Figure 1 plotted are the experimental data of k_{scc} for methane in aqueous solutions of alkali chlorides (LiCl, NaCl, KCl, RbCl, and CsCl) and of sodium halides (NaF, NaCl, NaBr, and NaI) against the ionic radii of cations and anions, respectively. This is an example of general non-monotonic behaviors of k_{scc} for the series of alkali metal ions with a common anion.[4]

There are several explanations for the origin of the exceptional behavior of Li^+ or, more generally, for the non-monotonic behavior of k_{scc} in the cation series.[11,15–18] In the present study we revisit this question and examine the ion size dependences of k_{scc} based on theory of liquid mixtures and computer simulation.

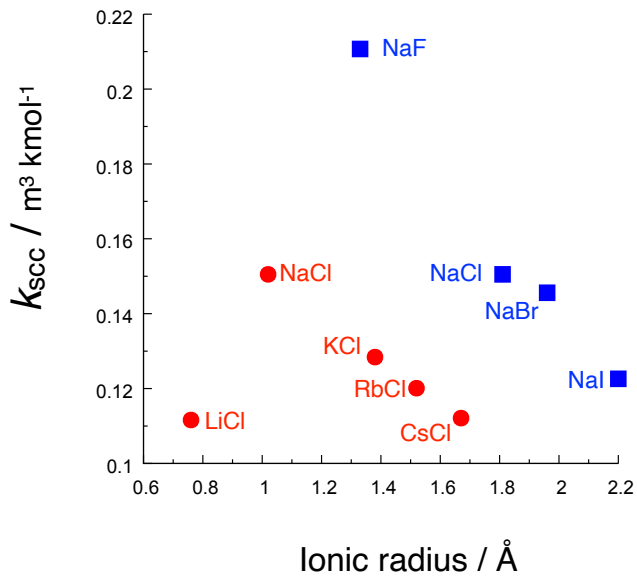

Figure 1: Setschenow coefficients[4] $k_{\rm scc}$ for methane in aqueous solutions of alkali chloride against the ionic radii of the alkali metal ions Li^+, Na^+, K^+, Rb^+, and Cs^+ (circles) and of sodium halides against the ionic radii of the halide ions F^-, Cl^-, Br^-, and I^- (squares). The ionic radii is taken from ref 20.

Theoretical background

The effect of ions on the solubility of a solute species in aqueous solution may be described by theory of liquid mixtures or more specifically by fluctuation theory: there is an extensive literature on this subject.[21–23] We start with the ratio ρ_i/z_i of the number density ρ_i to the activity z_i of species i and call it λ_i. Here, for non-dissociable species, z_i is defined such that in the ideal-gas limit $z_i \to \rho_i$; For salt species $X_{\nu_+}Y_{\nu_-}$ which dissociates into $\nu_+X^{z_+}$ and $\nu_-Y^{z_-}$ in solution, z_i is defined so as to become $\rho_X^{\nu_+}\rho_Y^{\nu_-} = \nu_+^{\nu_+}\nu_-^{\nu_-}\rho_i^{\nu_+ + \nu_-}$ in the ideal-gas limit. The solvation free energy μ_i^* of a non-dissociable solute in solution is then $\mu_i^* = -kT\ln\lambda_i$, with T the temperature and k Boltzmann's constant. When the solution is in equilibrium with its vapor, λ_i is essentially the solubility of solute i measured as the Ostwald absorption coefficient, for $\rho_i/z_i \simeq \rho_i/\rho_i^{\rm gas}$. From thermodynamic identities and statistical mechanics, one finds an exact relation for the rate of the change of $\ln\lambda_i$ with the activity z_j of another

component j at fixed temperature T, pressure p, and activities $z'_{j,k}$ of all species except j and k:

$$\frac{1}{\lambda_j}\left(\frac{\partial \ln \lambda_i}{\partial z_j}\right)_{T,p,z'_{j,k}} = G_{ij} - G_{ik}, \tag{2}$$

where G_{ij}, for example, is a measure of the fluctuation in N_i and N_j the numbers of molecules of species i and j in a macroscopic volume

$$G_{ij} = \frac{1}{\rho_i}\left[\frac{\langle \delta N_i \delta N_j \rangle}{\langle N_j \rangle} - \delta_{ij}\right] = \int h_{ij}(r) d\tau,$$

where $\delta N = N - \langle N \rangle$, δ_{ij} the Kronecker's delta, and $h_{ij}(r)$ the pair correlation function: the correlation function integrals are called the Kirkwood-Buff integrals.[24] The constraint of fixed $z'_{j,k}$ means the system is open for all molecular species except j and k. Changing the variable z_j in eq 2 to ρ_j and taking the limit $\rho_j \to 0$, one has, for non-dissociable species j,

$$\left(\frac{\partial \ln \lambda_i}{\partial \rho_j}\right)_{T,p,z'_{j,k}} = G_{ij} - G_{ik} \qquad (\rho_j \to 0). \tag{3}$$

When component j is a salt species dissociating into $\nu_+ \mathrm{X}^{z_+}$ and $\nu_- \mathrm{Y}^{z_-}$, one has instead

$$\left(\frac{\partial \ln \lambda_i}{\partial \rho_j}\right)_{T,p,z'_{j,k}} = (\nu_+ + \nu_-)(G_{ij} - G_{ik}) \qquad (\rho_j \to 0). \tag{4}$$

If the partial derivatives of eqs. 2, 3, and 4 are taken at fixed T and fixed activities z'_j of all species except j, G_{ik}'s on the right hand sides disappear.

The Setschenow equation 1 is the first-order approximation to an expansion of $\ln \lambda_{\mathrm{A}}$ of solute A in powers of the number density ρ_{s} of salt s at fixed T and with some additional constraints C

$$\ln \lambda_{\mathrm{A}} = \ln \lambda^0_{\mathrm{A}} - K_s \rho_{\mathrm{s}} + \mathcal{O}(\rho_{\mathrm{s}}) \qquad (\rho_{\mathrm{s}} \to 0), \tag{5}$$

where $\lambda^0_{\mathrm{A}} = \lim_{\rho_{\mathrm{s}} \to 0} \lambda_{\mathrm{A}}$, the solubility of species A in the solution without salt species s. When the constraints C are of fixed p and fixed activities $z'_{\mathrm{w,s}}$ of all species except component w

and salt species s ($=\mathrm{X}_{\nu_+}\mathrm{Y}_{\nu_-}$),

$$K_s = -\lim_{\rho_\mathrm{s}\to 0}(\partial \ln \lambda_\mathrm{A}/\partial \rho_\mathrm{s})_{T,p,z'_{\mathrm{w,s}}}. \tag{6}$$

Then, from eqs 4 and 6,

$$K_s = (\nu_+ + \nu_-)(G_\mathrm{Aw} - G_\mathrm{As}) \qquad (\rho_s \to 0). \tag{7}$$

The "salting out" ($K_s > 0$), by salt s, of solute A means $G_\mathrm{Aw} > G_\mathrm{As}$ and vice versa. Eqs 3, 4, and 7 hold for any multi-component systems in the limit of infinite dilution of cosolvent j or salt s. Essentially the same relations have been derived for ternary systems at fixed T, p, and z_A.[23]

In principle, G_As represents any G_{As_i} when salt s dissociates into ionic species $\{\mathrm{s}_i^{z_i}\}$, because the electroneutrality condition in a macroscopic volume centered at a molecule of solute A requires that G_{As_i} be all the same. The same principle applies to G_ws. In practice, however, when G_{As_i} or G_{ws_i} are evaluated numerically from the corresponding correlation functions obtained by molecular simulation, they could be appreciably different for different $\mathrm{s}_i^{z_i}$. Furthermore, at infinite dilution limit of ions, G_{As_i} or G_{ws_i} may be computed independently for each ionic species s_i, and so they would be ion specific.[25]

Consider now a three-component aqueous solution consisting of w (water), s (salt $\mathrm{X}_{\nu_+}\mathrm{Y}_{\nu_-}$), and A (hydrophobic solute), and suppose the solution is infinitely dilute in solute A, which is essentially the case for nonpolar solutes. Then the constraints with which ρ_s is varied is simply of fixed T and p, i.e., $K_s = -\lim_{\rho_s\to 0}(\partial \ln \lambda_i/\partial \rho_s)_{T,p}$. In this limit, $G_\mathrm{Aw} = -v_\mathrm{A}^*$, i.e., the negative of the solvation volume $v_\mathrm{A}^* \equiv v_\mathrm{A} - kT\chi$ of solute A, where χ is the isothermal compressibility of water and v_A the partial molecular volume of A, so that eq 7 is now

$$K_s = -(\nu_+ + \nu_-)(v_\mathrm{A}^* + G_\mathrm{As}) \qquad (\rho_s \to 0, \quad \rho_i \to 0). \tag{8}$$

The solvation volume v_{A}^{*} is the volume change that would be observed when a molecule of species A is added at a fixed point in the system; for the solvation of hydrophobic solutes in water near room temperature, $v_{\mathrm{A}}^{*} \simeq v_{\mathrm{A}} > 0$. Therefore, the salting out ($K_s > 0$) of a hydrophobic solute occurs when G_{As} is negative with its magnitude larger than the solvation volume v_{A}^{*}.

From eq 8 it follows that the salt effect as measured by K_s for a given hydrophobic solute comes from G_{As} alone. So we will examine G_{As} for various ions in order to understand the ion specific effects including the non-monotonic behavior of K_s with the size of alkali metal ions. There is another way of understanding the ion specific effects. It has been pointed out[11,14,15,17] that the ion specificity of the Setschenow coefficients K_s or the Hofmeister effects for a hydrophobic solute may be understood from how structure of water is affected by ions, i.e., from structural properties of electrolyte aqueous solutions. This point of view is naturally inferred from mean-field theory of liquid applied to hydrophobic hydration:[26,27] the changes in the solvation free energy with temperature, pressure, and salt concentration are mainly determined by the density or the packing fraction of the solution. Therefore, we shall examine volumetric properties of salt solutions, i.e., the packing fractions and the partial molar volumes of salts (or G_{ws}) for model electrolyte aqueous solutions and how they are correlated with the ion specificity of the Setschenow coefficients K_s.

Computational details

Macroscopic and microscopic properties of model aqueous solutions are obtained from molecular dynamics (MD) simulations. We performed NpT-ensemble MD simulations using the program package GROMACS[28] with the time step of 1 fs and the Nosé-Hoover method for the pressure-temperature control. All the MD simulations are performed at 298 K and 1 bar. Equilibrium configurations are sampled every 50 steps in the production run that follows the equilibration run. The duration of the production run ranges from 10 ns to 450 ns depending

on structural properties to be calculated and the equilibrium run is carried out at least 5 ns. The simulation cell is a cubic box with periodic boundary conditions. The three kinds of model systems, pure water, aqueous solutions of salt, and those of salt and methane, are prepared and simulated: each contains 2000 water molecules, 36 pairs of monovalent cations and anions are added for the model electrolyte solutions, so that the concentration of salt is 1.0 mol kg^{-1}, and 24 methane molecules are included for the solutions of salt and methane.

The potential function for the intermolecular interactions of water molecules is of the TIP4P/2005.[29] The potential functions for the ion-ion and ion-water interactions are the sum of the Lennard-Jones (LJ) and Coulomb potentials. Sodium and Chloride ions, Na^+ and Cl^-, are chosen to be the reference cation and anion. The force-field parameters of the ions are those proposed by Kohagen, Mason, and Jungwirth:[30,31] $\sigma_{Na} = 0.2115$ nm, $\epsilon_{Na} = 0.544284$ kJ/mol; $\sigma_{Cl} = 0.378240$ nm, $\epsilon_{Cl} = 0.4184$ kJ/mol. The ion models belong to a family of recently developed force fields that effectively incorporate polarization effects by scaling ionic charges. Methane molecules are modeled as the united atom LJ particles with the energy and size parameters:[32,33] $\epsilon_2 = 1.2301$ kJ/mol and $\sigma_2 = 0.373$ nm; The LJ parameters for methane-ion pairs are those given by the Lorentz-Berthelot combining rules; those for methane-water oxygen pairs are $\epsilon_{12} = 1.043$ kJ/mol and $\sigma_{12} = 0.34445$ nm.[34] The LJ potential part of all the intermolecular pair potentials is truncated at 0.9 nm and the long-range Coulomb interaction is calculated by the Ewald sum with the real-space cutoff of 0.9 nn. The set of the model potentials employed here reproduces accurately the density of pure water[29] and the solubility of methane in water[34] in a wide range of temperatures at 1 bar. We will see below that the calculated Setschenow coefficient of NaCl for the solubility of methane is very close to the experimental value, which shows that the recently developed charge-scaled force field for Na^+ and Cl^-[30,31] with the TIP4P/2005 water is more satisfactory in this regard than other common force fields.[34]

Two series of model salts including the reference salt NaCl are examined: one is the cation series in which only the LJ size parameters σ_+ of cations differ from each other while

the anion is fixed to be Cl^-; the other is the anion series in which only anions' σ_- differ from each other while the cation is fixed to be Na^+. The LJ energy parameters ϵ_+ and ϵ_- for cations and anions are always those of Na^+ and Cl^-, respectively. The force field parameters of the model salts are listed in Table I. Numbers followed by ionic species in the parentheses indicate that the LJ size parameters are chosen to be those of the ions; otherwise, the LJ size parameters of model ions are hypothetical ones.

Table 1: Lennard-Jones size parameters σ_+ and σ_- for the cation and anion series of the model salts. Numbers followed by symbols of ionic species in the parentheses indicate that σ_+ or σ_- is of that ionic species.

Cation series	1(Li^+)	2	3(Na^+)	4	5	6(K^+)	7	8(Cs^+)	9
σ_+ (nm)	0.18	0.2	0.2115	0.225	0.24	0.2838	0.33	0.3601	0.41
d (nm)	0.072	0.096	0.108	0.124	0.140	0.188	0.232	0.264	0.308

Anion series	1	2	3	4	5	6	7	8(F^-)	9(Cl^-)
σ_- (nm)	0.16	0.18	0.2115	0.24	0.27	0.30	0.33	0.3619	0.41
d (nm)	0.0041	0.032	0.068	0.104	0.136	0.168	0.196	0.228	0.276
Anion series	10	11(I^-)	12						
σ_- (nm)	0.44	0.4681	0.50						
d (nm)	0.300	0.324	0.352						

Also listed in table I are effective hard-sphere diameters d of ions

$$d = 2r_c - \sigma_{\mathrm{O}},$$

where r_c is the distance at which the ion-water(oxygen) radial distribution function becomes 1 on approach to the first maximum with increasing distance; σ_{O} is the LJ size parameter for the oxygen site of the TIP4P/2005 model. The effective diameters d for cations and anions will be used for the calculation of the packing fraction of model electrolyte solutions.

The solvation free energy μ^*_{A} of methane is calculated by the Widom test particle insertion method.[35] The test particle is inserted 2×10^5 times for each of 10^5 simulated equilibrium configurations with 50 fs intervals of pure water or aqueous solutions of salt. The Kirkwood-Buff

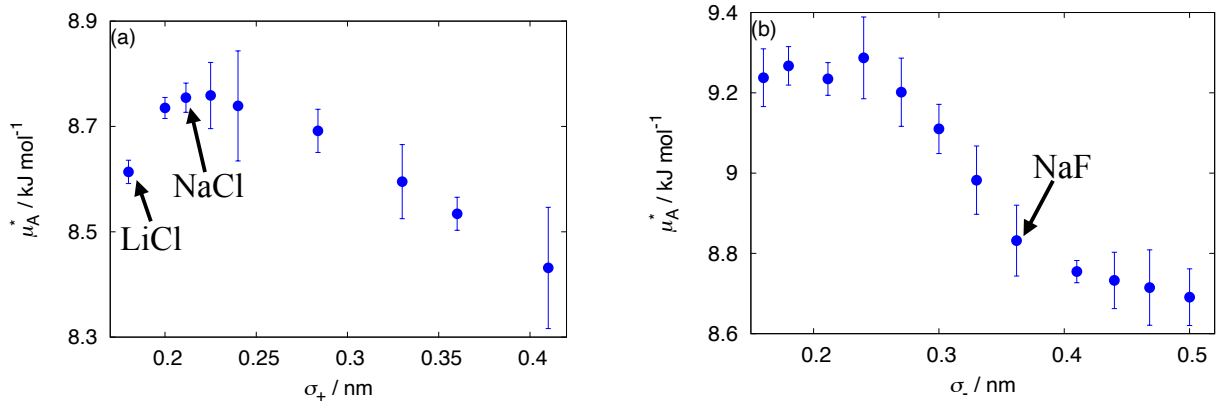

Figure 2: Ion size dependence of the solvation free energy μ_{A}^{*} of methane in the model electrolyte solutions: (a) cation series with the common anion Cl^{-}; (b) anion series with the common cation Na^{+}.

integrals G_{Aw}, G_{As}, and G_{ws} are evaluated from numerical integration of the corresponding pair correlation functions. MD trajectories of 450 ns are used to compute G_{Aw} and G_{As} and those of 150 ns are used for G_{ws}. The G_{As} are taken to be the average of $G_{\mathrm{As+}}$ and $G_{\mathrm{As-}}$, the solute-cation and solute-anion Kirkwood-Buff integrals.

Results and discussion

Ion size dependences of K_s

Figure 2 shows cation- and anion-size dependences of the solvation free energies μ_{A}^{*} of methane in model electrolyte aqueous solutions. In the cation series (fig 2a), μ_{A}^{*} is maximal at around σ_{+} of Na^{+} and rather sharply decreases as σ_{+} decreases to 0.18 nm, the value of Li^{+}. In the anion series (fig 2b), μ_{A}^{*} monotonically increases with decreasing σ_{-} up to $\sigma_{-} \simeq 0.25$ nm and plateaus out at smaller σ_{-}. Note that σ_{-} of the smallest anion F^{-} is 0.36 nm so that the salting-out effect of methane by halogen anions with the common cation Na^{+} decreases monotonically with the anion size. The above results for the cation and anion series are in accord with those reported by Docherty et al.[15]

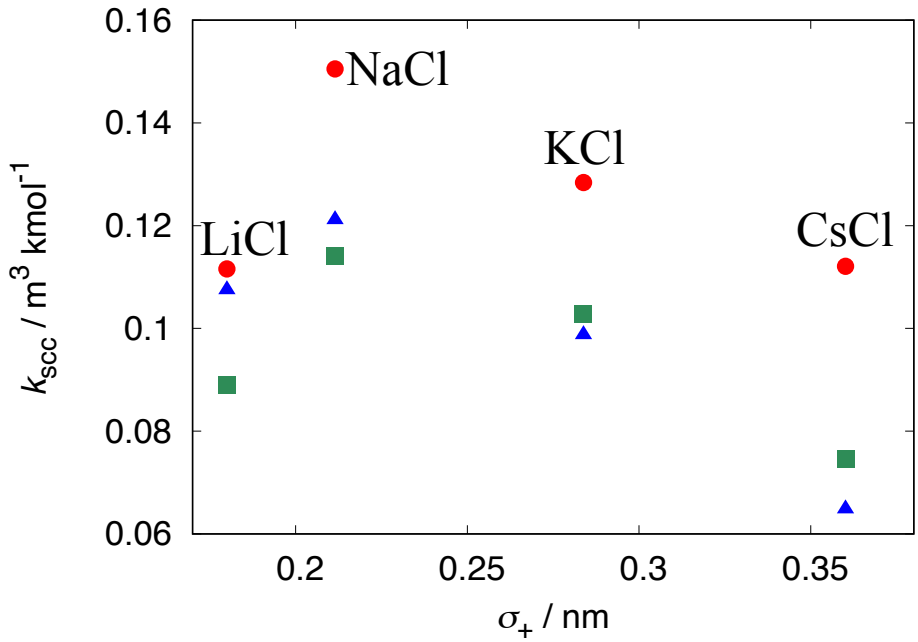

Figure 3: Computed Setschenow coefficients $k_{\rm scc}$ for the cation series of model aqueous solutions: eq 9 (squares) and eq 7 (triangles); Experimental data for LiCl, NaCl, KCl, and CsCl aqueous solutions of methane are also plotted as a reference (circles).

We evaluate the Setschenow coefficients K_s in two ways. One way is to use the linear approximation:

$$K_s = \lim_{\rho_s \to 0} \left(\frac{\partial \mu_{\rm A}^* / kT}{\partial \rho_s} \right)_{T,p} \simeq \frac{\mu_{\rm A}^* - \mu_{\rm A,0}^*}{\rho_s kT} \tag{9}$$

where $\mu_{\rm A}^*$ and $\mu_{\rm A,0}^*$ are the solvation free energies of methane in salt solution and in pure water, respectively, at infinite dilution of methane: $\mu_{\rm A}^*$ and $\mu_{\rm A,0}^*$ were evaluated by applying the test-particle insertion to methane-free salt solutions and pure water. Another way is to use eq 7 (or eq 8) with $G_{\rm Aw}$ and $G_{\rm As}$ (or $v_{\rm A}^*$) at infinite dilution of methane and salt, where the subscripts A, w, and s denote methane, water and salt, respectively. In this method, both $G_{\rm Aw}$ and $G_{\rm As}$ are evaluated from numerical integration of the pair correlation functions obtained from MD simulations of aqueous solutions of methane and salt. The approximation involved in this method is that $G_{\rm Aw}$ and $G_{\rm As}$ at low but finite concentrations of methane and salt are taken to be those at the infinite dilution limit.

Figure 3 shows the Setschenow coefficients $k_{\rm scc}$ (converted from K_s) for the cation series: plotted are two sets of numerical results (eq 9 with the test-particle insertion method and eq 7 with the numerical integration of the correlation functions) together with experimental data for LiCl, NaCl, KCl, and CsCl aqueous solutions. It is seen that the numerical results from the two routes are in good agreement with each other, both giving the largest $k_{\rm scc}$ at σ_+ of Na^+. The computed values of $k_{\rm scc}$ for NaCl (0.114 m^3/kmol) via eqs 7 and 9 underestimate by 20% and 24%, respectively, the experimental value; the deviation is significantly smaller than, and in opposite direction from, earlier results[15,36] obtained for common force fields of NaCl,[37,38] which suggests that the charge-scaling force field of NaCl[30,31] with the TIP4P/2005 model water is more accurate in describing the salting-out effect in aqueous solutions. Note that the computed Setschenow coefficients in figure 3 are systematically smaller than the experimental data in spite of the fact that the TIP4P/2005 water with the LJ methane accurately reproduces the solvation free energy of methane in aqueous solution without ions. Thus, the deviations are likely due to the model potentials for ion-water interactions, more specifically, those for the chloride ion-water interaction. But the present models suffice in order to investigate the reversed order of sodium and lithium ions in the salting-out effect.

The ion size dependence of the Setschenow coefficient K_s arises from that of $G_{\rm As}$ alone (eq 7 or 8), and so the observation that K_s (LiCl) $<$ K_s (NaCl) reflects the fact that $G_{\rm As}$ is more negative in the NaCl solution than in the LiCl solution. In other words, the result illustrates the plain fact that the more repulsive the solute-ion effective interaction the more strongly the solubility of the solute is reduced by the salt. The question is then why the effective interaction between methane and Li^+ is less repulsive than that between methane and Na^+.

Ion size dependences of the packing fraction of solution and the partial molar volume of electrolytes

It has been pointed out in earlier computational studies[15,17,39] that the Setschenow coefficients of electrolyte solutions are correlated with volumetric properties of the solutions such as the packing fractions, the partial molar volumes of the ions, or the volume contraction caused by electrostriction.

The packing fraction η of a model solution is defined by

$$\eta = \frac{\pi}{6} \sum_i \rho_i d_i^3, \tag{10}$$

where ρ_i is the average number density of species i in the system and d_i the effective hard-sphere diameter of that species, the sum being taken over all species. The values of d_i for model cations and anions are listed in Table 1 and that for water is taken to be the LJ size parameter of the oxygen site in the TIP4P/2005 model. In Figure 4 the packing fractions η of the cation and anion series of the solutions are plotted against the ion diameters σ_+ or σ_-. In the cation series, η is maximal at around the ion size of Na^+ while in the anion series η increases monotonically with decrease in σ_- over the whole range. The non-monotonic and monotonic behaviors of η for the cation and anion series, respectively, correspond to those of μ_{A}^* (Figure 4).

Ion-specificity in packing fractions of electrolyte solutions is closely related to that in partial molar volumes of electrolytes, for both reflect the degree of electrostriction. Relation between ion-specific electrostriction and partial molar volumes of electrolytes in solvents is thoroughly discussed in ref. 40. The partial molecular volume v_{s} of an electrolyte in water at infinite dilution is directly related to G_{ws} via one of the Kirkwood-Buff relations: $v_{\mathrm{s}} = kT\chi - G_{\mathrm{ws}}$, with χ now the isothermal compressibility of water. Note also that $v_{\mathrm{s}} \simeq -G_{\mathrm{ws}}$ for most cases: e.g., at 298 K, 1 bar, $v_{\mathrm{s}} \simeq 17$ cm^{3}mol^{-1} for NaCl while $kT\chi \simeq 1.1$ cm^{3}mol^{-1} for pure water. Therefore, the correlation between η and v_{s} is essentially that between η and

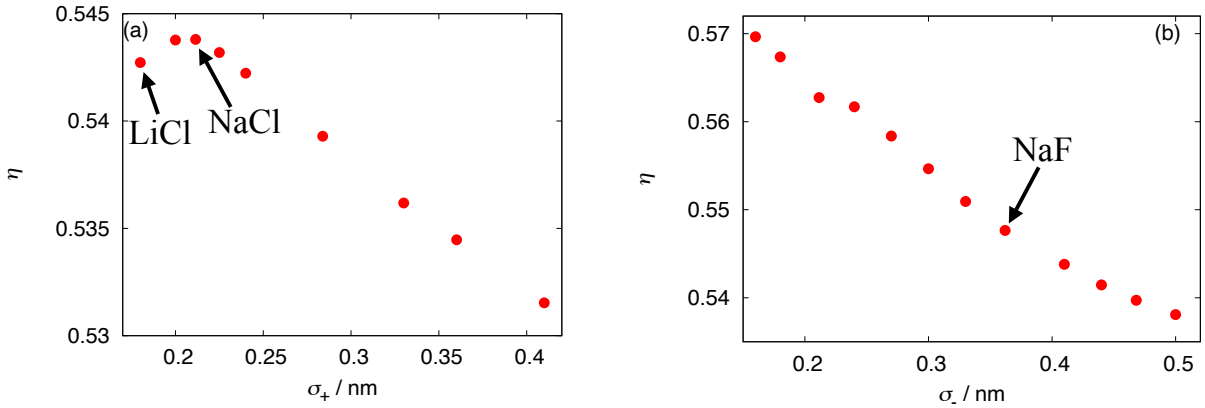

Figure 4: Ion size dependences of the packing fraction η of the model electrolyte solutions: (a) cation series with the common anion Cl^-; (b) anion series with the common cation Na^+.

$G_{\rm ws}$. Figure 5 shows $G_{\rm ws}$ against η for six model electrolyte solutions. There is a near linear correlation between η and $G_{\rm ws}$.

Microscopic origins of the ion size dependences of η and $v_{\rm s}$

Effect of formation of ion clusters

Ion pairings and cluster formation of ions in some aqueous solutions have been directly observed in computer simulations[41–44] and have been studied by experiment.[45,46] Thomas and Elcock argued that formation of ion strings in simulated LiCl aqueous solutions is a potential explanation for the exceptional behavior of lithium salts.[16] Therefore, a plausible microscopic mechanism of the non-monotonic cation size dependences of η and $v_{\rm s}$ in the cation series with a common anion species is that as the cation size decreases there appears a growing tendency to form clusters or strings of ions, thereby reducing the degree of electrostriction. In the snapshots of our MD simulations, we observe some associations of ions when the cation size is of Li^+. To examine the possible effect of ion associations we performed additional MD simulations in which the cation-anion LJ size parameters are deliberately set to be a large value, 0.6 nm, so that each ion is fully hydrated and has no chance of forming ion clusters. This setting is similar, in practice, to the constraint used in ref. 16

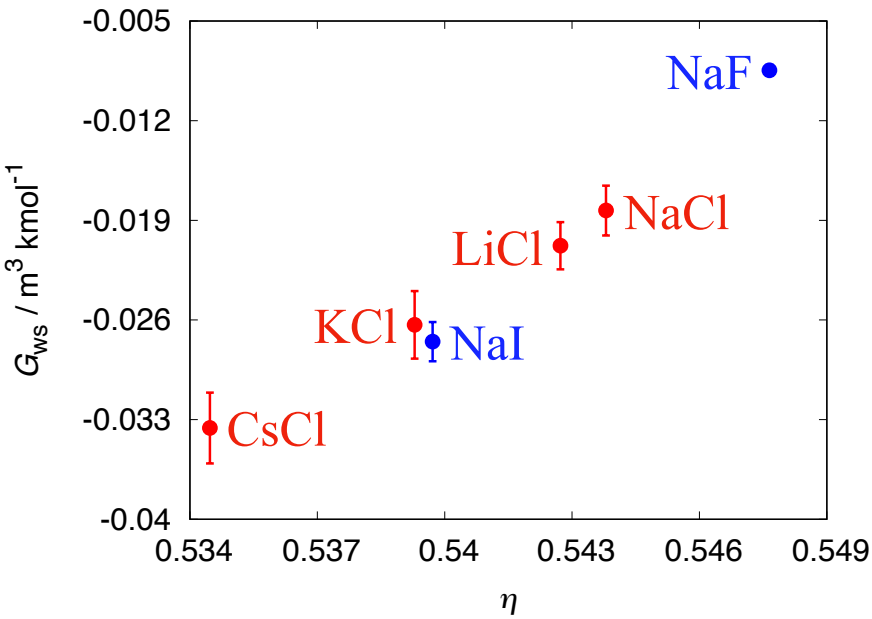

Figure 5: Ion specific η vs. $G_{\rm ws}$ for the selected model electrolyte solutions in Table I.

Figure 6 shows the results for the system with ion associations suppressed together with those for the original ones. As shown in Figure 6a, the cation size dependence of η for the system with no ion associations is virtually the same as that for the original system. Therefore, the decrease of η and the increase of $v_{\rm s}$ with decreasing cation size from that of Na^+ cannot be explained by associations of ions. It is also seen in Figure 6b that the solvation free energy $\mu_{\rm A}^*$ of methane in the model electrolyte solutions with no ion association is maximal at a cation size close to that of Na^+ as it is in the solutions with no constraint. Therefore, the anomalous behavior of lithium salts regarding the salting-out effect should be explained without resort to formation of ion clusters.

Local packing structure around each ion

In order to reveal microscopic mechanisms of the anomalous ion-size dependences of the packing fraction η of the solution and the partial molecular volume $v_{\rm s}$ of salt s for the cation series, we examine the following integrals of the ion-water pair correlation functions $h_{\rm ws\pm}(r)$

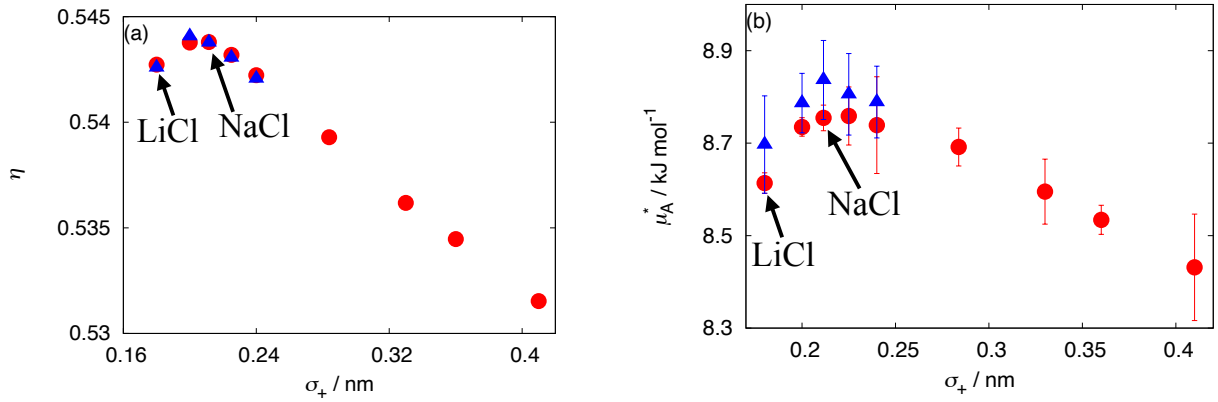

Figure 6: Effects of ion associations on cation size dependences of (a) the packing fraction η and (b) the solvation free energy μ_{A}^* of methane in the cation series: electrolyte solutions with ion associations suppressed (triangles) and those with no constraint (circles).

as a function of the upper limit R of the integral:

$$G_{\mathrm{ws}\pm}(R) = 4\pi \int_0^R h_{\mathrm{ws}\pm}(r) r^2 dr \qquad (+ \text{ for cations}, - \text{ for anions}). \tag{11}$$

For an infinitely dilute solution, $-G_{\mathrm{ws}\pm}(R)$ is the contribution to the solvation volume $v_{\mathrm{s}}^* = v_{\mathrm{s}} - kT\chi$ of salt s from the sphere of radius R, centered at a cation or an anion.

Figure 7a shows $G_{\mathrm{ws}+}(R)$ for selected cation sizes. The pair correlation functions employed here are those between oxygen and ion species. It can be seen that the orders of $G_{\mathrm{ws}+}(R)$ at the second maxima, at the third minima, and at the following extrema are the same as the order of $G_{\mathrm{ws}+}(\infty)$, indicating that the origin of the anomalous behaviors of v_{s} and η for the cation series should lie in the spherical solvation volume of that radius ~ 0.5 nm around each cation. In fig. 7b the first maximum and the second minimum of $G_{\mathrm{ws}+}(R)$ are plotted against the cation size σ_+. It is shown that the first maximum decreases with σ_+ whereas the second minimum increases with σ_+. This means that the water density of the first hydration shell increases as the cation size decreases, but the density of water in the volume of a spherical shell adjacent to the first shell decreases with decreasing σ_+. These opposing behaviors of the two regions result in the appearance of the minimum partial molec-

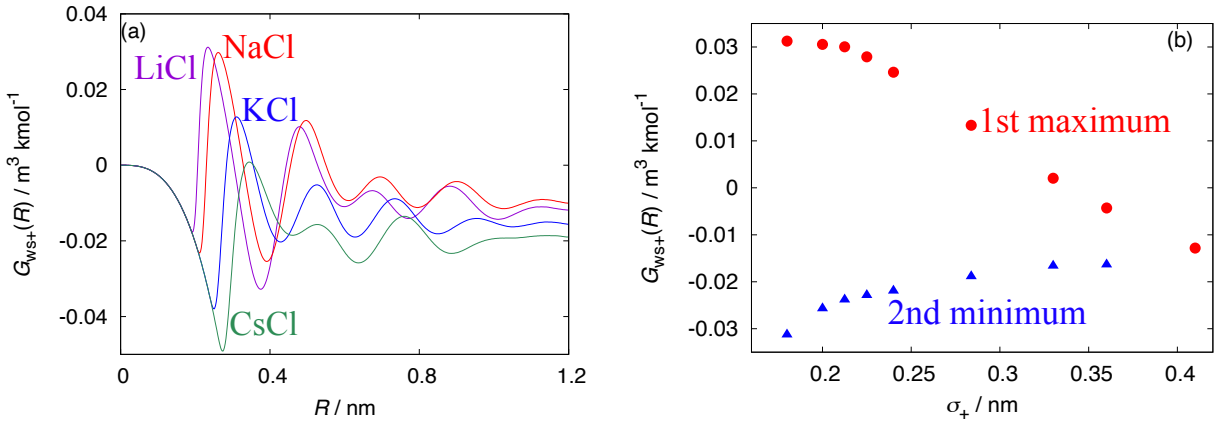

Figure 7: (a) $G_{\mathrm{ws+}}(R)$ for the four cations Li^+, Na^+,K^+, and Cs^+ in the cation series; (b) the first maximum and the second minimum of $G_{\mathrm{ws+}}(R)$ against the cation size σ_+ in the cation series.

ular volume and the maximum packing fraction at the cation size close to that of Na^+. In Figure 8 shown are $G_{\mathrm{ws-}}(R)$ for selected anion sizes and the first maximum and the second minimum of $G_{\mathrm{ws-}}(R)$ against the anion size σ_-. For the three anions whose size is of F^-, Cl^-, and I^-, the order of $G_{\mathrm{ws-}}(R)$ at any common extremum is the same as the order of $-v_{\mathrm{s}}^*$ (Figure 8a), and actually that is true for all the anions in the anion series. Figure 8b shows that the first maximum and the second minimum both decrease monotonically with decreasing σ_-. These results explain the regular behaviors of v_{s} and η for the anion series.

We have found that the spherical solvation volume of radius ~ 0.5 nm around each cation basically determines the anomalous behavior of v_{s} for the cation series. It is also possible to identify the spherical volume around each ion that determines the packing fraction η of electrolyte solutions. To do so, first, we define the solvation packing fraction $\eta(R)$ to be the packing fraction in the spherical region of radius R centered at a solvated ion. We calculate $\eta(R)$ using the radial distribution functions $g_i(r)$ for pairs of the central ion and species i $(=\mathrm{w}, \mathrm{s+}, \mathrm{s-})$:

$$\eta(R) = \frac{\pi}{2R^3} \sum_i \rho_i d_i^3 \int_0^\infty f(r; R, d_i/2) g_i(r) r^2 dr + \left(\frac{d_{\mathrm{s}}}{2R}\right)^3, \quad (R > d_{\mathrm{s}}/2) \tag{12}$$

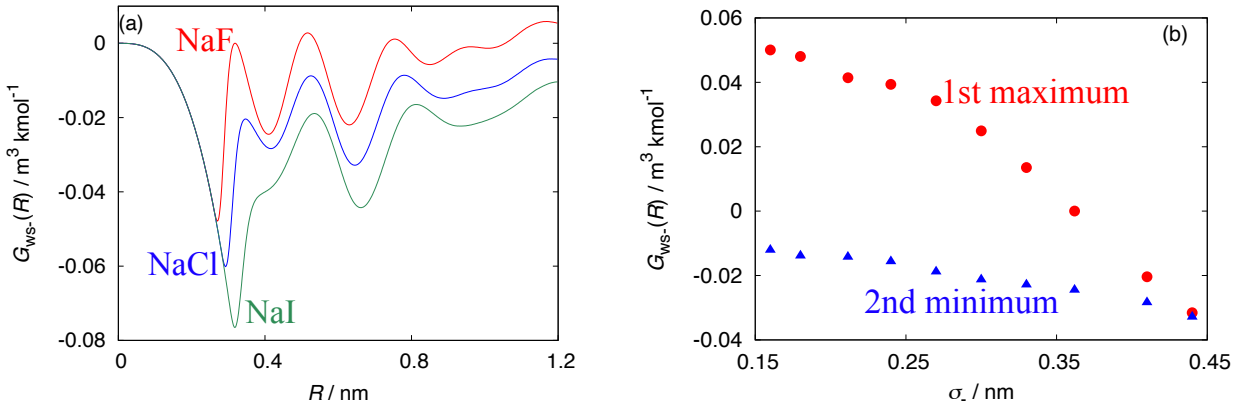

Figure 8: (a) $G_{\mathrm{ws}-}(R)$ for the three anions F^-, Cl^-, and I^- in the anion series; (b) the first maximum and the second minimum of $G_{\mathrm{ws}-}(R)$ against the cation size σ_- in the anion series.

where $f(r; R, d_i/2)$ is the fraction of the volume of intersection of two spheres of radii R and $d_i/2$ with the center-center distance r to the volume of the sphere of radius $d_i/2$; d_{s} is the effective hard-sphere diameter of the central ion. We have calculated $\eta(R_1)$, $\eta(R_2)$, and $\eta(R_3)$ for the first, the second, and the third solvation spheres of radii R_n ($n = 1, 2, 3$): Here R_n is taken to be the distance of the n-th local minimum of the ion-water(oxygen) radial distribution function.

Figure 9 shows the solvation packing fractions around cations in the cation series and those around anions in the anion series. In the cation series (Figure 9a), $\eta(R_1)$ increases monotonically with decrease in σ_+, and so as regards the first solvation shell, the smaller the cation the larger the degree of electrostriction. However, $\eta(R_2)$ and $\eta(R_3)$ for the second and the third solvation spheres both exhibit a maximum around the size of Na^+, indicating that the anomalous behavior of η of the electrolyte solutions in the cation series is manifested in the second solvation sphere centered at a cation. In the anion series (Figure 9b), $\eta(R_1)$, $\eta(R_2)$, and $\eta(R_3)$ all increase with decrease in σ_- as does η and the smaller the solvation sphere the larger the rate of change in $\eta(R_n)$ with σ_-. No anomalous behavior is found in any solvation spheres in the anion series.

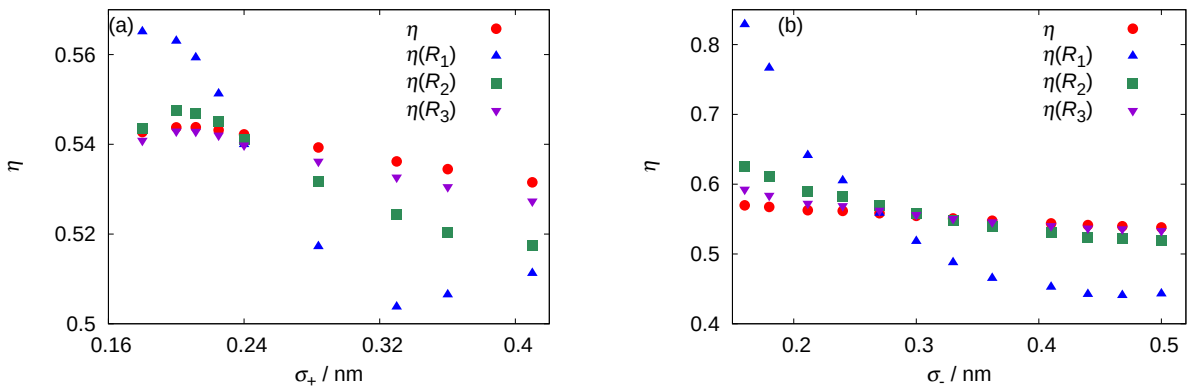

Figure 9: The solvation packing fractions $\eta(R_n)$ for the first, the second, and the third solvation spheres of radii R_n $(n = 1, 2, 3)$ and the bulk packing fraction η, against (a) cation sizes σ_+ in the cation series and (b) anion sizes σ_- in the anion series.

Molecular orientation and packing in solvation spheres around an ion

Given the fact that the ion-size dependences of v_s and η are monotonic in the anion series and non-monotonic in the cation series, microscopic origins of that difference must be sought for in the molecular orientations of water with respect to a central cation and anion. Here we define θ to be the angle between the dipole moment of H_2O and the vector from the oxygen atom to a central ion as shown in Figure 10a, and now we shall examine the orientations $\cos\theta$ of the molecular dipoles.

Figures 10b and 10c show distributions of the average orientation $\langle\cos\theta\rangle$ of water molecules in the first solvation shells of cations and anions. For the selected cations in the cation series, the peak position of the distribution shifts significantly toward more negative values as the cation size decreases whereas in the anion series the peak position shifts only slightly toward more positive values with decrease in σ_-. The different ion-size dependences of the distributions of $\langle\cos\theta\rangle$ between cations and anions may be explained as follows. Water molecules in the first solvation shell around cations tend to orient to face their oxygen atoms toward cations and the tendency continuously increases as the cation size goes down to Li^+. By contrast, one OH group from each water molecule around an anion is more or less locked in

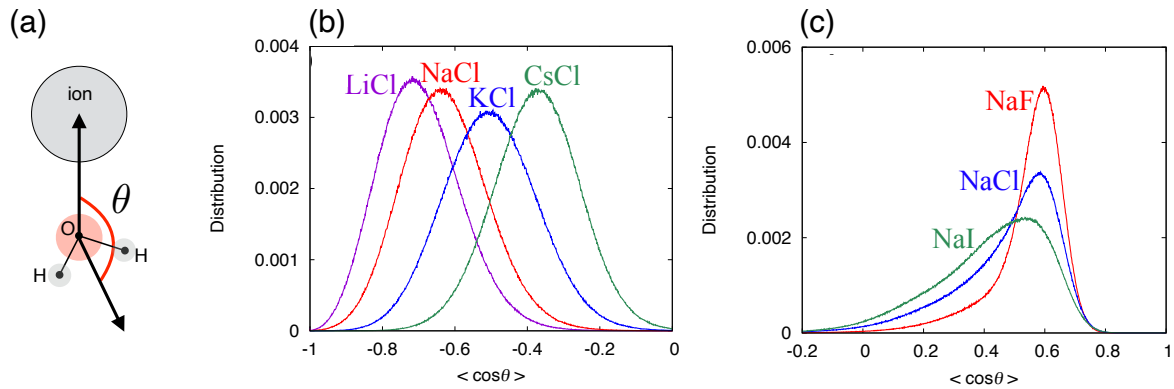

Figure 10: (a) Definition of angle θ; (b), (c) Distributions of $\langle \cos\theta \rangle$ for water molecules in the first solvation shell around each cation (b) and anion (c).

a state where the O−H and the anion are aligned straight, and therefore the peak position of the $\langle \cos\theta \rangle$ distribution is only weakly dependent on the anion size.

We calculated the *conditional* solvation packing fraction $\eta(R_n; \langle \cos\theta \rangle)$, the packing fraction around each ion averaged over the simulated configurations having a prescribed value of $\langle \cos\theta \rangle$. Figure 11 displays $\eta(R_2; \langle \cos\theta \rangle)$ for the second solvation spheres of cations (Figure 11a) and anions (Figure 11b). In each case of cations, $\eta(R_2; \langle \cos\theta \rangle)$ depends significantly on $\langle \cos\theta \rangle$ with a maximum at some value of $\langle \cos\theta \rangle < 0$. In particular, $\eta(R_2; \langle \cos\theta \rangle)$ for Li^+ and Na^+ are very similar to each other and both decrease sharply as $\langle \cos\theta \rangle$ goes to -1, i.e., as all the water molecules in the first solvation shell tend to orient their oxygen atoms toward a central cation. But as we have seen in Figure 10 the peak position of the distribution of $\langle \cos\theta \rangle$ of Li^+ is closer to -1 than that of Na^+, so that the solvation packing fraction $\eta(R_2)$ is lower around Li^+ than around Na^+. Since the order of η for the cation series is determined by that of $\eta(R_2)$ (Figure 9), the observation above concerning Figures 10b and 11a seems to be the microscopic origin of the non-monotonic ion-size dependences of η and v_s for the cation series. On the other hand, in the anion series, $\eta(R_2; \langle \cos\theta \rangle)$ for each anion has no strong dependence on $\langle \cos\theta \rangle$ and the smaller the ion size the larger $\eta(R_2; \langle \cos\theta \rangle)$ (Figure 11b), so that one observes simple, monotonic ion-size dependences of v_s and η for the anion series.

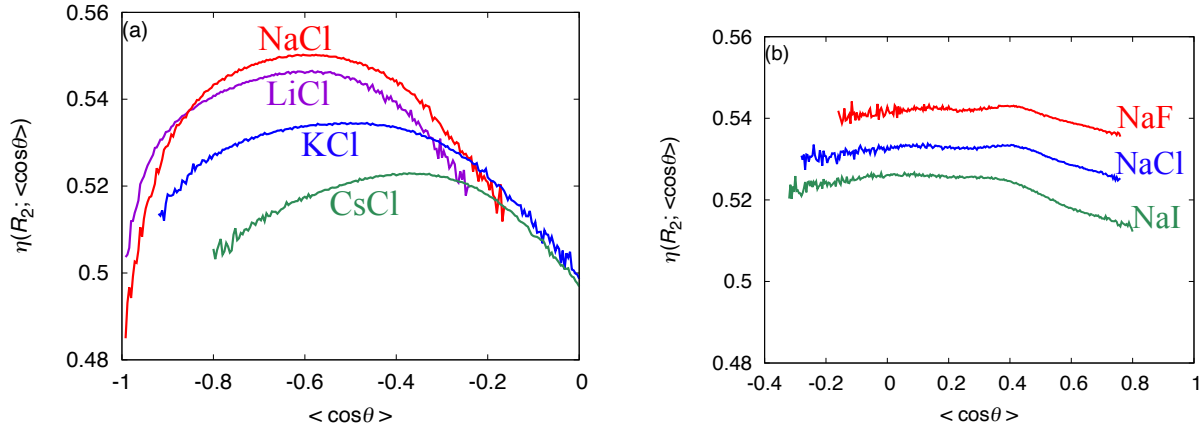

Figure 11: The conditional solvation packing fractions $\eta(R_2; \langle\cos\theta\rangle)$ for the second solvation spheres of (a) cations and (b) anions, as functions of $\langle\cos\theta\rangle$.

Relation between G_{As} and G_{ws}

As observed in earlier studies[15,17] and shown in the present work for the cation and anion series (Figures 2 and 4), the Setschenow coefficients K_s or the solvation free energies μ^*_{A} of a hydrophobic solute in electrolyte aqueous solutions are correlated with the packing fractions η or the partial molecular volumes v_{s} of salts in those solutions. But the observed correlations are by no means trivial because the former is a property of aqueous solutions of salts alone while the latter is the one concerning both salts and solutes. This means that in terms of the Kirkwood-Buff integrals there must be some correlation between G_{As} and G_{ws} because the ordering of ions in K_s is due to that of G_{As} and the ordering in η (or v_{s}) comes from G_{ws}. In Figure 12 is shown G_{As} vs. G_{ws} for the selected salt aqueous solutions in the cation and anion series. As anticipated, there is a strong correlation between G_{As} and G_{ws}: a linear fit to the data gives $G_{\mathrm{As}} = -6.4G_{\mathrm{ws}} - 0.45$.

CONCLUSIONS

Ion size dependences of the salting-out effect for the cation and anion series were contrasted and the origins of the differences were examined.

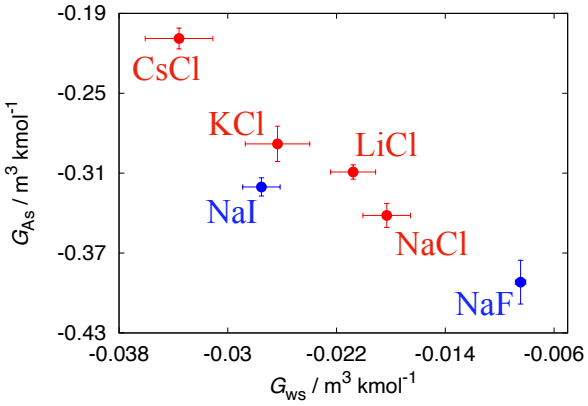

Figure 12: Correlation between G_{As} and G_{ws} for model salts in the cation and anion series.

In the cation series where the cation size is varied while the anion is fixed to be Cl^-, the solvation free energy μ_{A}^* of methane is maximal at around the cation size σ_+ of Na^+ and decreases rather sharply as σ_+ decreases further. In the anion series where the anion size is varied, μ_{A}^* is a monotonic function of the anion size σ_-.

The Setschenow coefficients K_s in the cation series were calculated from two different routes, eq 8 with the test-particle insertion method and eq 6 with the correlation-function integrals. The two sets of the results are similar to each other and show that the reverse order of Li^+ and Na^+, in agreement with experimental data.[4]

The correspondence between the salting-out effect and volumetric properties of electrolyte aqueous solutions were confirmed. The packing fraction η and the partial molar volume v_{s} of salt show non-monotonic dependences on σ_+ in the cation series while they are monotonic functions of σ_- in the anion series.

Microscopic origins of the ion-size dependences of μ_{A}^*, η and v_{s} were examined. First, it is demonstrated that formation of ion clusters in aqueous solutions of LiCl is not responsible for the reverse order of lithium and sodium ions in the ion size dependences of μ_{A}^* and η. Second, we calculated the ion-water pair correlation function integrals $G_{\mathrm{ws}\pm}(R)$ as a function of the radius R of the spherical volume centered at each ion in the cation and anion series. A notable conclusion derived from the calculation is that the spherical volume of radius

$\sim$ 0.5 nm around each cation sets the order of cations for $G_{\rm ws} \simeq -v_{\rm s}$ including the reverse order of lithium and sodium salts. Third, we also calculated the solvation packing fractions $\eta(R_1)$, $\eta(R_2)$, and $\eta(R_3)$ for the first, second, and third solvation spheres around a cation and an anion. It is found that $\eta(R_1)$ increases monotonically with decreasing σ_+ but $\eta(R_2)$ and $\eta(R_3)$ show maxima at around σ_+ of Na^+, thereby confirming that the second solvation sphere sets the tendency of the non-monotonic behavior of η in the cation series. In the anion series, $\eta(R_1)$, $\eta(R_2)$, and $\eta(R_3)$ all increases monotonically with decreasing σ_-. Fourth, we examined the distribution of the average orientation $\langle \cos\theta \rangle$ of water molecules in the first solvation shell of each ion species and the conditional solvation packing fraction $\eta(R_2; \langle \cos\theta \rangle)$ for the second solvation spheres, and found the following microscopic mechanism. The peak position of the distribution of $\langle \cos\theta \rangle$ shifts significantly toward -1 with decreasing σ_+ in the cation series; $\eta(R_2; \langle \cos\theta \rangle)$ for Li^+ and Na^+ are similar to each other and decrease sharply as $\langle \cos\theta \rangle$ goes to -1; and thereby $\eta(R_2)$ for Li^+ is smaller than that for Na^+.

Finally, relation between the Setschenow coefficients of methane and the volumetric properties of aqueous solutions was examined in terms of the Kirkwood-Buff integrals $G_{\rm ws}$ and $G_{\rm As}$. A near linear correlation between $G_{\rm ws}$ and $G_{\rm As}$ was found for the model electrolyte solutions including both the cation and anion series. Qualitatively, the correlation is consistent with the commonly observed results: the higher the packing fraction of the aqueous solution the lower the solubility of a hydrophobic solute.[11,14,15,17,26,27] The following question remains to be answered: How robust is the correlation between $G_{\rm ws}$ and $G_{\rm As}$? The present study considered the size effect of monovalent ions alone. It is interesting to examine, among variety of ionic species, which groups of ions form a more-or-less universal $G_{\rm ws}$-$G_{\rm As}$ curve and which fall off from it. Furthermore, there is no reason to expect a simple correlation between $G_{\rm ws}$ and $G_{\rm As}$ when solute species are not simple hydrophobic ones but those with hydrophilic moieties, i.e., when the solubilities are determined by both the shape of a solute molecule and the specific interactions with solvent molecules and ions. Clarifying the robustness of the $G_{\rm ws}$-$G_{\rm As}$ correlation is a subject of future study.

ACKNOWLEDGMENTS

This work was supported by JSPS KAKENHI (Grant Nos. 18KK0151, 18K03562, and 20H02696).

References

(1) Long, F. A.; McDevit, W. F. Activity Coefficients of Nonelectrolyte Solutes in Aqueous Salt Solutions. *Chem. Rev.* **1952**, *51*, 119–169.

(2) Clever, H. L. Sechenov Salt-Effect Parameter. *J. Chem. Eng. Data* **1983**, *28*, 340–343.

(3) Schumpe, A. The estimation of gas solubilities in salt solutions. *Chemical Engineering Science* **1993**, *48*, 153–158.

(4) Weisenberger, S.; Schumpe, A. Estimation of gas solubilities in salt solutions at temperatures from 273 K to 363 K. *Aiche Journal* **1996**, *42*, 298–300.

(5) Jungwirth, P.; Cremer, P. S. Beyond Hofmeister. *Nat. Chem.* **2014**, *6*, 261–263.

(6) Zhang, Y.; Cremer, P. S. Interactions between macromolecules and ions: The Hofmeister series. *Curr Opin Chem Biol* **2006**, *10*, 658–663.

(7) Shimizu, S.; McLaren, W. M.; Matubayasi, N. The Hofmeister series and protein-salt interactions. *J. Chem. Phys.* **2006**, *124*, 234905.

(8) Pegram, L. M.; Record, M. T. Thermodynamic origin of hofmeister ion effects. *J. Phys. Chem. B* **2008**, *112*, 9428–9436.

(9) Lo Nostro, P.; Ninham, B. W. Hofmeister Phenomena: An Update on Ion Specificity in Biology. *Chem. Rev.* **2012**, *112*, 2286–2322.

(10) Okur, H. I.; Hladílková, J.; Rembert, K. B.; Cho, Y.; Heyda, J.; Dzubiella, J.; Cremer, P. S.; Jungwirth, P. Beyond the Hofmeister Series: Ion-Specific Effects on Proteins and Their Biological Functions. *J. Phys. Chem. B* **2017**, *121*, 1997–2014.

(11) Kinoshita, M.; Hirata, F. Analysis of salt effects on solubility of noble gases in water using the reference interaction site model theory. *J. Chem. Phys.* **1997**, *106*, 5202–5215.

(12) Smith, P. E. Computer Simulation of Cosolvent Effects on Hydrophobic Hydration. *J. Phys. Chem. B* **1999**, *103*, 525–534.

(13) Kalra, A.; Tugcu, N.; Cramer, S. M.; Garde, S. Salting-In and Salting-Out of Hydrophobic Solutes in Aqueous Salt Solutions. *J. Phys. Chem. B* **2001**, *105*, 6380–6386.

(14) Hribar, B.; Southall, N. T.; Vlachy, V.; Dill, K. A. How Ions Affect the Structure of Water. *J. Am. Chem. Soc.* **2002**, *124*, 12302–12311.

(15) Docherty, H.; Galindo, A.; Sanz, E.; Vega, C. Investigation of the Salting Out of Methane from Aqueous Electrolyte Solutions Using Computer Simulations. *J. Phys. Chem. B* **2007**, *111*, 8993–9000.

(16) Thomas, A. S.; Elcock, A. H. Molecular Dynamics Simulations of Hydrophobic Associations in Aqueous Salt Solutions Indicate a Connection between Water Hydrogen Bonding and the Hofmeister Effect. *J. Am. Chem. Soc.* **2007**, *129*, 14887–14898.

(17) Graziano, G. On the Salting Out of Benzene by Alkali Chlorides. *J Chem Eng Data* **2009**, *54*, 464–467.

(18) Ganguly, P.; Hajari, T.; van der Vegt, N. F. A. Molecular Simulation Study on Hofmeister Cations and the Aqueous Solubility of Benzene. *J. Phys. Chem. B* **2014**, *118*, 5331–5339.

(19) Setschenow, J. Über die Konstitution der Salzlösungen auf Grund ihres Verhaltens zu Kohlensäure. *Zeitschrift für Physikalische Chemie* **1889**, *4*, 117–125.

(20) Shannon, R. D. Revised Effective Ionic Radii and Systematic Studies of Interatomie Distances in Halides and Chaleogenides. *Acta Cryst.* **1976**, *A32*, 751–767.

(21) Ruckenstein, E.; Shulgin, I. Salting-Out or -In by Fluctuation Theory. *Ind. Eng. Chem. Res.* **2002**, *41*, 4674–4680.

(22) Ben-Naim, A. *Molecular Theory of Solutions*; Oxford: New York, 2006.

(23) Smith, P. E.; Mazo, R. M. On the Theory of Solute Solubility in Mixed Solvents. *J. Phys. Chem. B* **2008**, *112*, 7875–7884.

(24) Kirkwood, J. G.; Buff, F. P. The statistical mechanics theory of solutions. I. *J. Chem. Phys.* **1951**, *19*, 774–777.

(25) Schnell, S. K.; Englebienne, P.; Simon, J.-M.; Krüger, P.; Balaji, S. P.; Kjelstrup, S.; Bedeaux, D.; Bardow, A.; Vlugt, T. J. H. How to apply the Kirkwood–Buff theory to individual species in salt solutions. *Chem. Phys. Lett.* **2013**, *582*, 154–157.

(26) Abe, K.; Sumi, T.; Koga, K. Mean-Field Approximation to the Hydrophobic Hydration in the Liquid–Vapor Interface of Water. *J. Phys. Chem. B* **2016**, *120*, 2012–2019.

(27) Koga, K.; Yamamoto, N. Hydrophobicity Varying with Temperature, Pressure, and Salt Concentration. *J. Phys. Chem. B* **2018**, *122*, 3655–3665.

(28) Hess, B.; Kutzner, C.; van der Spoel, D.; Lindahl, E. GROMACS 4: Algorithms for Highly Efficient, Load-Balanced, and Scalable Molecular Simulation. *J. Chem. Theory Comput.* **2008**, *4*, 435–447.

(29) Abascal, J. L. F.; Vega, C. A general purpose model for the condensed phases of water: TIP4P/2005. *J. Chem. Phys.* **2005**, *123*, 234505.

(30) Kohagen, M.; Mason, P. E.; Jungwirth, P. Accurate Description of Calcium Solvation in Concentrated Aqueous Solutions. *J. Phys. Chem. B* **2014**, *118*, 7902–7909.

(31) Kohagen, M.; Mason, P. E.; Jungwirth, P. Accounting for Electronic Polarization Effects in Aqueous Sodium Chloride via Molecular Dynamics Aided by Neutron Scattering. *J. Phys. Chem. B* **2016**, *120*, 1454–1460.

(32) Guillot, B.; Guissani, Y. A Computer Simulation Study of the Temperature Dependence of the Hydrophobic Hydration. *J. Chem. Phys.* **1993**, *99*, 8075–8094.

(33) Hirschfelder, J. O.; Curtiss, C. F.; Bird, R. B. *Molecular Theory of Gases and Liquids*; Wiley: New York, 1954; pp 348–353.

(34) Docherty, H.; Galindo, A.; Vega, C.; Sanz, E. A potential model for methane in water describing correctly the solubility of the gas and the properties of the methane hydrate. *J. Chem. Phys.* **2006**, *125*, 074510.

(35) Widom, B. Some topics in the theory of fluids. *J. Chem. Phys.* **1963**, *39*, 2808–2812.

(36) The estimated value of k_s is 60% larger than the experimental value. It is also confirmed that common nonpolarizable force fields for salts with no charge scaling overestimate the salting out effect on methane.

(37) Smith, D. E.; Dang, L. X. Computer simulations of NaCl association in polarizable water. *J. Chem. Phys.* **1994**, *100*, 3757–3766.

(38) Joung, I. S.; Cheatham, T. E. I. Determination of Alkali and Halide Monovalent Ion Parameters for Use in Explicitly Solvated Biomolecular Simulations. *J. Phys. Chem. B* **2008**, *112*, 9020–9041.

(39) Holzmann, J.; Ludwig, R.; Geiger, A.; Paschek, D. Temperature and Concentration Effects on the Solvophobic Solvation of Methane in Aqueous Salt Solutions. *ChemPhysChem* **2008**, *9*, 2722–2730.

(40) Mazzini, V.; Craig, V. S. J. What is the fundamental ion-specific series for anions

and cations? Ion specificity in standard partial molar volumes of electrolytes and electrostriction in water and non-aqueous solvents. *Chem. Sci.* **2017**, *8*, 7052–7065.

(41) Degrève, L.; Mazzé, F. M.; 2003, Molecular simulation of LiCl aqueous solutions. *Mol. Phys.* **2003**, *101*, 1443–1453.

(42) Hassan, S. A. Computer Simulation of Ion Cluster Speciation in Concentrated Aqueous Solutions at Ambient Conditions. *J. Phys. Chem. B* **2008**, *112*, 10573–10584.

(43) Fennell, C. J.; Bizjak, A.; Vlachy, V.; Dill, K. A. Ion Pairing in Molecular Simulations of Aqueous Alkali Halide Solutions. *J. Phys. Chem. B* **2009**, *113*, 6782–6791.

(44) Pluharova, E.; Mason, P. E.; Jungwirth, P. Ion Pairing in Aqueous Lithium Salt Solutions with Monovalent and Divalent Counter-Anions. *J. Phys. Chem. A* **2013**, *117*, 11766–11773.

(45) Antonio, M. R.; Nyman, M.; Anderson, T. M. Direct Observation of Contact Ion-Pair Formation in Aqueous Solution. *Angew. Chem. Int. Ed.* **2009**, *48*, 6136–6140.

(46) Bian, H.; Wen, X.; Li, J.; Chen, H.; Han, S.; Sun, X.; Song, J.; Zhuang, W.; Zheng, J. Ion clustering in aqueous solutions probed with vibrational energy transfer. *Proc. Natl. Acad. Sci. USA* **2011**, *108*, 4737–4742.
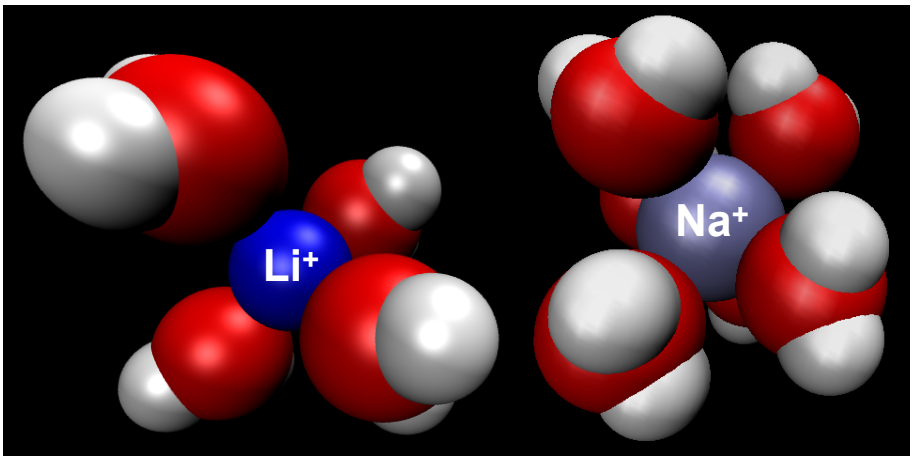
Table of Contents - Graphic